Quantitative Driver Acceptance Modeling for Merging Car at Highway Junction and Its Application to the Design of Merging Behavior Control

Hiroyuki Okuda, *Member, IEEE*, Tatsuya Suzuki, *Member, IEEE*, Kota Harada, Shintaro Saigo, and Satoshi Inoue

***Abstract*— This study models the decision-making characteristics of a driver regarding whether he accepts a merging car at a highway junction. Then, the application of the modeling to the design of merging behavior control is proposed. First, the driving behavior on the main lane at a highway junction is observed using a driving simulator, particularly focusing on the driver's state of decision (SOD), which represents the acceptance for merging a car coming from the merging lane. Second, the driver's SOD is modeled using a logistic regression model and the prediction performance of the identified model is verified. Finally, the speed controller of the merging car is designed to maximize the acceptance from the cars on the main lane. The key idea here is to minimize the entropy of the SOD of the driver on the main lane by optimizing the speed of a merging vehicle. This problem is quantitatively formulated using an identified decision-making model and addressed by applying a randomized approach to the optimization. This enables the automated vehicle to realize a considerate merging behavior at a highway junction. Numerical experiments are performed to demonstrate the usefulness of the proposed design scheme.**

***Index Terms*— Driver model, merging behavior, model predictive control.**

I. Introduction

DEVELOPMENT of driving intelligence for the design of an advanced driver assistance system and/or an automated driving system is attracting remarkable attention. The complexity of driving intelligence increases particularly when considering interaction with other vehicles, because the so-called "consensus" mechanism must be achieved in real time with limited information. Although the difficulty of designing this consensus mechanism highly depends on the availability of vehicle-to-vehicle (V2V) communication technology, V2V communication is unlikely to be available in all cars in the near future.

Merging behavior at a highway junction is a typical task that requires consensus among cars. In this task, a consensus must be accomplished in a particularly short time range to prevent accidents and/or traffic congestion. The difficulty of realizing such a prompt consensus is highly evident when V2V communication is not available. Meanwhile, human drivers naturally make a consensus with the drivers of other cars by appropriately considering the behavior of these cars without V2V communication. Particularly, consideration of the decision-making characteristics of other drivers is also important. Hence, implementing such a considerate consensus mechanism on an automated merging car is highly recommended.

Merging behavior has already been investigated in many literatures. [1]–[5] analyzed the merging behavior by focusing on a driver's operation in a merging car. [6]–[8] also attempted to model a merging behavior for traffic flow analysis and simulations. Many types of driver assistance and partial/completely automated lane merging systems have also been discussed to reduce the burden of a driver from the control technology perspective [9]–[17]. However, these studies mainly focused on the physical safety index rather than the achievement of a consensus among cars.

The decision-making characteristics of a driver in the merging car is analyzed in [18]–[21]. These analyses are useful to reproduce a precise merging behavior. However, the decision-making characteristics of the driver in the main lane must be focused and analyzed for the consensus mechanism design. This perspective is quite useful for the design of an automated merging car.

The most significant aim of this study is to exploit the decision-making model of other drivers in the controller design. This perspective has never been investigated before and will be a fundamental principle in the controller design of an automated car in an "interactive situation" with other cars. Based on these backgrounds, this study aims to verify the concept of consensus making with other cars at an interactive situation, particularly focusing on a conflicting scenario during the merging task with limited and controlled factors.

First, the driving behavior on the main lane at the highway junction is observed using a driving simulator (DS), particularly focusing on a driver's acceptance for the merging car coming from a merging lane. Second, the driver's acceptance is modeled using a logistic regression model and the prediction performance of the identified model is verified.

Finally, a design scheme of the merging behavior control of a car on the merging lane is proposed. The proposed control scheme comprises two-stage controls. The first one is to realize

Manuscript received February 5, 2018; revised December 26, 2018 and June 7, 2019; accepted November 6, 2019. The Associate Editor for this article was C. Wu. *(Corresponding author: Hiroyuki Okuda.)*

H. Okuda, T. Suzuki, and K. Harada are with Department of Mechanical systems Engineering, Nagoya University, Aichi 464-8603, Japan (e-mail: h_okuda@nuem.nagoya-u.ac.jp).

S. Saigo and S. Inoue are with Toyota Motor Corporation, Toyota City 471-8571, Japan.

Digital Object Identifier 10.1109/TITS.2019.2957391

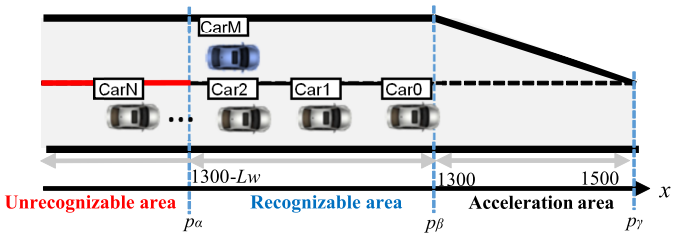

Fig. 1. Merging task at a highway junction.

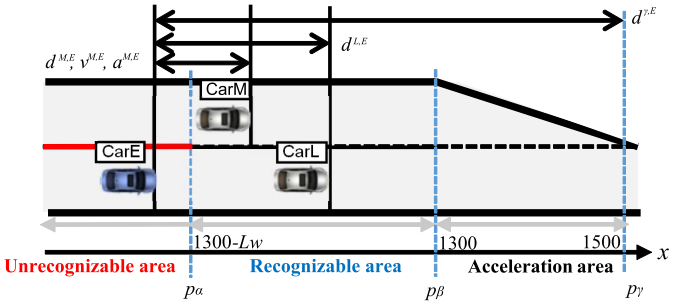

Fig. 2. Measurement of driving behavior on the main lane.

a fast consensus with the cars on the main lane by optimizing the speed (consensus control). The key idea in this stage is to minimize the entropy of the state of decision (SOD) of the drivers on the main lane by optimizing the speed of the merging vehicle. By exploiting this idea in a model predictive control (MPC) framework, the vagueness of the decision-making of the drivers on the main lane is reduced. This scheme is quantitatively formulated using the identified SOD model and realized by applying sampling-based MPC, referred to as randomized MPC (RMPC). The second one is to finalize the merging task after making consensus in the first stage (merging control). Owing to the consensus mechanism in the first stage, the control difficulty in the second stage is reduced. The proposed control mechanism enables an automated vehicle to realize a considerate merging behavior at a highway junction. Particularly, the validity of the proposed design scheme is demonstrated via numerical experiments.

II. Driving Behavior Modeling on the Main Lane

A. Target Task and Problem Setting

The final goal of this study is to design a control strategy of the merging behavior on the merging lane at a highway junction shown in Fig.1. In the target environment, N cars (labeled by Car 1 to Car N) are supposed to run on a straight main lane following Car 0 without any lane change. Thereafter, one merging car, Car M , approaches the highway ramp and cuts in between cars on the main lane.

When we observe the merging behavior of the human driver, he predicts the behavior of the cars on the main lane to achieve the merging task safely and smoothly. From this perspective, we assume that the decision-making and motion control characteristics of the drivers on the main lane play an important role in the design of a merging behavior, which must be represented using a rigorous mathematical model.

B. Definition of State of Acceptance

Figure 2 presents the definition of variables that characterize the decision-making of a driver in Car E (ego car). These variables play important roles in modeling the decision-making characteristics of the driver of Car E whether he accepts the cut-in of the Car M in front of Car E or not. To formalize the decision-making characteristics, the state of decision(SOD) is defined as follows:

State of decision ($X_{SOD} \in \{1, 2, 3\}$)

1) $X_{SOD} = 1$: *ACCEPT*
   Driver of Car E allows Car M to cut-in in front of Car E .
2) $X_{SOD} = 2$: *REJECT*
   Driver of Car E DOES NOT allow Car M to cut-in in front of Car E .
3) $X_{SOD} = 3$: *UNDECIDED*
   Driver of Car E is yet to decide *ACCEPT* or *REJECT*.

The SOD of Car E at the moment when Car M appears is *UNDECIDED* ($X_{SOD}(0) = 3$). As Car E approaches the end of the merging lane, the SOD is whether to "accept" or "reject" depending on the relative behavior of the merging vehicle. However, the SOD is not observable in real-time applications. Therefore, we must develop a mathematical model for estimating the SOD.

Considering that the SOD has a stochastic variance, using a model that has a probability measure is preferred. In this study, the probability measure of the SOD of the driver in Car E is modeled using a logistic regression model. The output of the logistic regression model is the probability of each state of the driver in Car E . The input, that is, explanatory variables of the model, is defined by $\phi(t)$. The probability of each state in this model, $P(X_{SOD}(t) = s|\phi(t))(s =\in \{1, 2, 3\})$, is calculated using a logistic function, which is also referred to as a soft-max function. The most probable state is estimated using the maximum of the probability of each state, as follows:

$$\begin{aligned} X_{SOD}(t) &= \arg\max_s P(X_{SOD}(t) = s|\phi(t)) \\ &= \arg\max_s P_s(\phi(t)), \end{aligned} \tag{1}$$

$$P_s(\phi(t)) = \begin{cases} \dfrac{\exp(\eta_s^T\phi(t))}{1+\exp(\eta_1^T\phi(t))+\exp(\eta_2^T\phi(t))}, & \text{if } s \in \{1,2\}, \\ 1 - P_1(\phi(t)) - P_2(\phi(t)), & \text{if } s = 3, \end{cases} \tag{2}$$

$$\phi(t) = \left(1,\ \mathbf{A}^E(t)^T,\ \mathbf{E}^E(t)^T\right)^T, \tag{3}$$

$$\mathbf{A}^E(t) = \left(d^{M,E}(t),\ v^{M,E}(t),\ a^{M,E}(t)\right)^T \in \mathbb{R}^3, \tag{4}$$

$$\mathbf{E}^E(t) = \left(d^{L,E}(t),\ d^{\gamma,E}(t),\ L_w\right)^T \in \mathbb{R}^3, \tag{5}$$

where t is the time index in discrete time, $X_{SOD}(t)$ is the SOD at time t, and $\phi(t)$ is the regressor vector comprising the variables shown in Fig. 2. Moreover, $\mathbf{A}^E$ is a variable set related to Car M , and its element is defined in Table I. Note that these variables are controllable by adjusting the approaching speed of Car M . Meanwhile, $\mathbf{E}^E$ consists of parameters depending on the configuration of a junction and

TABLE I
VARIABLE DEFINITION FOR SOD ESTIMATION

$d^{M,E}(=p^M-p^E)$	Distance between Car E and Car M
$v^{M,E}(=v^M-v^E)$	Relative speed between Car E and Car M
$a^{M,E}(=a^M-a^E)$	Relative acceleration between Car E and Car M
$d^{L,E}(=p^L-p^E)$	Distance between Car E and Car L
$d^{\gamma,E}(=p_\gamma-p^E)$	Relative distance to the end of the acceleration area
$L_w(=p_\beta-p_\alpha)$	Length of recognizable area

positions of Car E and Car L (Table I). The variables in $\mathbf{E}^E$ are not controllable from Car M, whereas $d^{L,E}(t)$ can be varied depending on the driving of Car L. Note that this modeling idea is applicable when many cars on the highway (such as trailing vehicles) are considered by adding some appropriate explanatory variables.

The parameter vector, $\eta_s (s \in \{1,2\})$, is estimated from a set of output and input variables, that is, the observed SOD and regressor vector. (Please see [22] for the identification detail of the logistic regression model.)

C. Overall Structure of the Driver Model on the Main Lane

The driver model of Car E comprises two parts, namely decision-making and motion control. The decision-making part, that is, SOD of Car E, is simulated using a logistic regression model, as stated in the previous section. Meanwhile, the motion control part expresses the acceleration/deceleration behavior of Car E based on three simple PD controllers assigned to each SOD. The overall structure of the driver model of Car E is formulated as follows:

$$y(t+1) = \begin{cases} f_{acc}(\phi(t)), & \text{if} \quad X_{SOD}(t)=1, \\ f_{rej}(\phi(t)), & \text{if} \quad X_{SOD}(t)=2, \\ f_{und}(\phi(t)), & \text{if} \quad X_{SOD}(t)=3, \end{cases} \tag{6}$$

$$X_{SOD}(t) = \arg\max_s \{P(X_{SOD}=s|\phi(t))\}, \tag{7}$$

where t is the time index in discrete time and $y(t+1)$, which is the output of the driver, is the acceleration of Car E at time $t+1$. In addition, ϕ is a regressor vector and $P(X_{SOD}=i|\phi(t))$ denotes the probability of each state calculated using (Eq. 2) when $\phi(t)$ is observed. This $P(X_{SOD}=i|\phi(t))$ is the decision-making model introduced in the previous section. This switched PD control model can be regarded as a specified model of the probability-weighted autoregressive exogenous model(PrARX model) proposed in [25]. The details of the applied PD control functions in each SOD are given as follows:

$$f_{acc}(\phi(t)) = G\Big(d_{\text{ref}}(1),\ \min(d^{L,E}(t),\ d^{M,E}(t)), \tag{8}$$

$$\min\Big(d^{L,E}(t-1),\ d^{M,E}(t-1)\Big)\Big), \tag{9}$$

$$f_{rej}(\phi(t)) = G\Big(d_{\text{ref}}(2),\ d^{L,E}(t),\ d^{L,E}(t-1)\Big), \tag{10}$$

$$f_{und}(\phi(t)) = G\Big(d_{\text{ref}}(3),\ d^{L,E}(t),\ d^{L,E}(t-1)\Big), \tag{11}$$

where $d^{i,j}(t)$ is the distance between Car i and Car j at time t. The function $G(d_{\text{ref}}, d_{\text{cur}}, d_{\text{prev}})$ denotes the acceleration control to follow the targeting car with reference distance d_{ref},

$$G\left(d_{\text{ref}}, d_{\text{cur}}, d_{\text{prev}}\right) = k_p\left(d_{\text{ref}}-d_{\text{cur}}\right)+k_d\left(d_{\text{prev}}-d_{\text{cur}}\right). \tag{12}$$

Fig. 3. DS used for the measurement.

Parameters $\theta = (d_{\text{ref}}(1),\ d_{\text{ref}}(2), and\ d_{\text{ref}}(3))^T$ are the reference distances of each model for *ACCEPT*, *REJECT*, and *UNDECIDED* modes, respectively. Furthermore, θ is determined from the experimental data by calculating the average of the corresponding reference distance in each SOD. Note that the parameter θ varies from driver to driver. Car L is the leading car when the SOD is *REJECT* or *UNDECIDED*. Meanwhile, the small distance from Car E to Car M or to Car L is regarded as the reference distance when the SOD is *ACCEPT*. Parameters k_d and k_p are used in the PD controller specified via trial and error, and are assumed to be common for all drivers.

The obtained model may not have a perfect accuracy for the car behavior prediction because of the simplicity of the model. The prediction of the driver's SOD is the key issue in the proposed method to compute the decision entropy, as explained in the latter part. Therefore, this study focuses on the decision-making part of the model rather than the motion control part. The prediction performance of SOD is verified in section II-F. Although the prediction accuracy of the closed-loop behavior of the overall model is not quantitatively discussed in this paper, we particularly assume that the proposed motion control model provides better prediction performance of the driving speed of Car E in short term, at least as compared to a standard single linear controller model. In addition, MPC, that is, a receding horizon control used in this study, updates the prediction by referring to the latest measurement in each control cycle [33]. The receding horizon control is known as the control scheme that provides better control performance than the optimal control if certain modeling errors occur. The validity of model prediction, including both decision-making and motion control parts, is verified through the validation of the entire proposed system in section IV-B.

D. Data Collection for Driver Modeling

First, the driving data are collected using a DS to identify the driver model. The DS used in this study is shown in Fig.3. It has three main screens to display frontal 180° angle of the horizontal view. A side screen providing the view from -90° (left) to -120° (left back) is added to obtain a wide view on the left side. In the DS, an actual dashboard is placed to emulate reality. Three small monitors are also attached at the room mirror, where the right and left door mirrors are designed to provide the rear views to the driver. The dynamics of the ego car motion is computed using the Carsim commercial software from Mechanical Simulation Inc.

TABLE II
INITIAL CONDITION IN THE MEASUREMENT OF Car M

Initial position	-20, -10, 0, +10, +20 [m]
Initial speed	60, 70,$\cdots$, 120 [km/h]
Initial acceleration	-0.1 ,0, +0.1 [m/s^2]
Length of recognizable area (p_α to p_β)	50, 150, 300 [m]

The simple straight expressway with two lanes, as shown in Fig. 2, is used as the driving environment for data collection to simplify the problem. The merging car, Car M , and Car L are driven automatically using a certain control algorithm explained later. The drivers are supposed to drive Car E by simply following the leading car, Car L , according to their usual driving. Some of the drivers' characteristics influencing the driving, such as the rushing situation and distraction caused by drowsiness and/or fatigue, are removed from our model to avoid complexity, leading to the intractability of the controller design.

A total of 28 drivers participated in this experiment and submitted informed consent prior to the experiment. Car L runs at a constant speed (22.22m/s) as usual driving. Prior to position p_α in Fig.2, the driver cannot see Car M because a tall noise barrier is present on its left side (referred to as unrecognizable area). After passing p_α, the noise barrier becomes low; hence, the driver can see Car M (referred to as recognizable area). The acceleration area starts from position p_β and ends at position p_γ. Car M starts moving after Car E passes 50[m] ahead from p_α and constantly moves along the predetermined driving path. Car M must change its driving lane to the main lane before the end of the merging lane.

Each driver (in Car E) drives 100 times with different approaching scenarios of Car M . Sixty experimental scenarios are randomly selected by changing the initial position, speed, and acceleration of Car M , as listed in Table II. Additional 20 approaching scenarios are generated by intentionally applying acceleration or deceleration to Car M between p_α and p_β to increase the number of scenarios. Furthermore, 20 more speed patterns are generated for Car M , which refers to the approaching profile of a human driver assuming that Car E and Car L drive at a constant speed (pre-experiments are performed for this task).

From the identification perspective, controlling the "input signal", i.e., speed pattern of Car M and Car L) is important to cover various driving scenarios. Particularly, we test 80 different driving scenarios to capture the natural driving behavior of the driver on Car E , as mentioned previously. Consequently, the explanatory variables of the model vary widely, which is sufficient for the identification process.

During the experiment, the variables listed in Table I are observed every $\Delta t = 100$ms. Given that the SOD is not directly observable in the standard setup of the cockpit, we attach a push button ("accept" or "reject") on the steering wheel, and the drivers are requested to push either the "accept" or "reject" button according to their SOD (Fig.4). If the driver decides to *ACCEPT* the merging of Car M in front of Car E , he pushes the "accept" button. The decision once made can be changed at any time during a trial depending on the behavior of Car M .

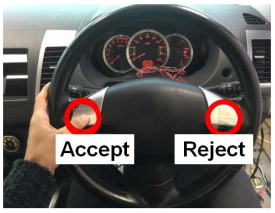

Fig. 4. Switches attached on the steering wheel.

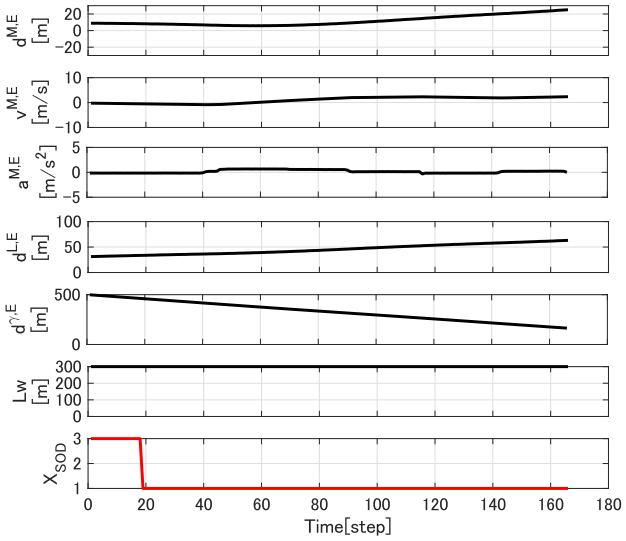

Fig. 5. Example of the measured data profile (*ACCEPT* case).

Examples of the observed data are shown in Figs.5 and 6. They illustrate the profiles when the driver *ACCEPT* and *REJECT* Car M , respectively. The horizontal axis represents time [step], whereas the vertical ones show the variables listed in Table I and the observed SOD. The data measurement starts when Car E passes point p_α and finishes when either Car E or Car M reaches point p_γ.

E. Samples of the Identified Driver Model

In this section, several samples of the identified driver model are discussed, particularly focusing on the SOD, i.e., the logistic regression model. The obtained driver model varies from driver to driver (personalized model). For convenience, the driver model for driver j ($j \in \{1, \cdots, 28\}$) is described by $\mathbf{M}^j = [\eta^{j^T}, \theta^{j^T}]^T$.

The identified parameters of the driver model for driver $j = 1$ and $j = 3$ are listed in Table III. In addition, the average and standard deviation of these parameters among all drivers are listed in Table IV. Note that the average and standard deviations are those of the parameters of all drivers and not the parameters of the average driver model, which is obtained from the measurement of all subjects shown in section IV-B. η_1 and η_2 are the parameters of the logistic regression model that specifies the switching condition of the state between *UNDECIDED* and *ACCEPT*and between *UNDECIDED* and *REJECT*, respectively. Given that all regressor

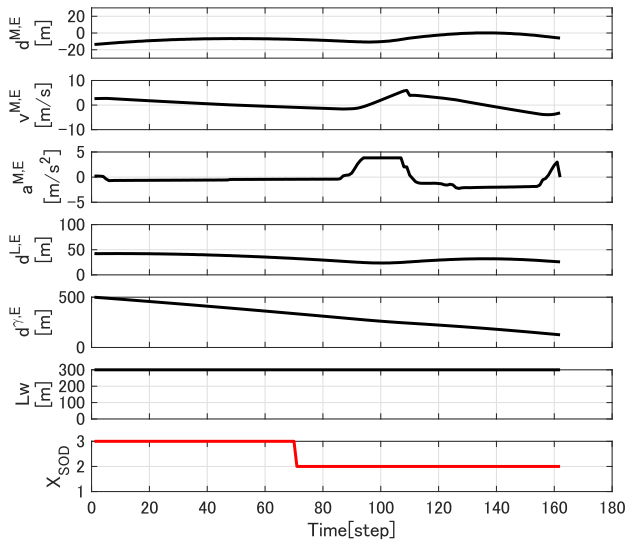

Fig. 6. Example of the measured data profile (*REJECT* case).

TABLE III
EXAMPLES OF THE OBTAINED PARAMETERS OF THE DRIVER MODEL

driver 1	const.	$d^{M,E}$	$v^{M,E}$	$a^{M,E}$	$d^{L,E}$	$d^{\gamma,E}$	L_w
η_1	5.87	6.70	2.38	0.27	0.36	-6.64	5.49
η_2	6.51	-1.05	-1.54	-0.83	-0.73	-6.77	6.34

driver 3	const.	$d^{M,E}$	$v^{M,E}$	$a^{M,E}$	$d^{L,E}$	$d^{\gamma,E}$	L_w
η_1	-0.75	4.32	0.53	1.04	1.31	-4.44	2.72
η_2	2.26	-1.67	-0.41	0.51	-0.94	-3.64	2.75

driver 1	$d_{\mathrm{ref}}(1)$	$d_{\mathrm{ref}}(2)$	$d_{\mathrm{ref}}(3)$
θ	47.6	38.1	37.8

driver 3	$d_{\mathrm{ref}}(1)$	$d_{\mathrm{ref}}(2)$	$d_{\mathrm{ref}}(3)$
θ	43.3	24.0	30.1

TABLE IV
AVERAGE AND STANDARD DEVIATIONS OF THE OBTAINED PARAMETERS

η_1	const.	$d^{M,E}$	$v^{M,E}$	$a^{M,E}$	$d^{L,E}$	$d^{\gamma,E}$	L_w
mean	-0.13	4.92	0.50	0.79	0.40	-3.28	1.21
std. dev.	3.06	1.82	0.61	0.57	0.58	2.18	1.56

η_2	const.	$d^{M,E}$	$v^{M,E}$	$a^{M,E}$	$d^{L,E}$	$d^{\gamma,E}$	L_w
mean	0.16	-0.95	-0.39	-0.28	-0.32	-3.32	1.24
std. dev.	2.52	1.29	0.68	0.54	0.51	1.82	1.74

θ	$d_{\mathrm{ref}}(1)$	$d_{\mathrm{ref}}(2)$	$d_{\mathrm{ref}}(3)$
mean	54.84	39.38	40.32
std. dev.	14.85	14.54	10.13

variables are normalized, the magnitude of these parameters represents the importance of the corresponding variables in the decision-making characteristics of the acceptance.

The results listed in Table III of driver $j = 1$ implies that $d^{M,E}$ (i.e., relative distance between Car E and Car M) plays the most important role in the decision on the acceptance of the merging of Car M. In addition, $v^{M,E}$ (i.e., relative speed between Car E and Car M) is more important to decide the rejection of merging than $d^{M,E}$. Meanwhile, the driver

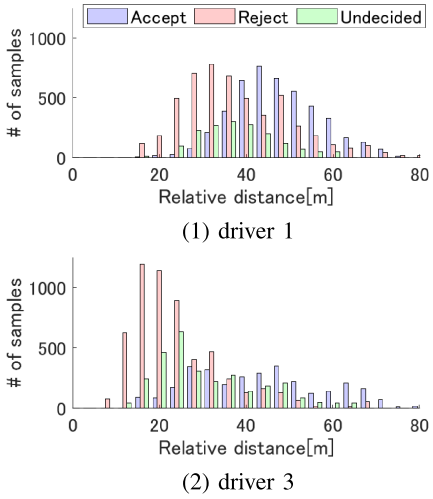

Fig. 7. Distribution of distance $d^{L,E}$ in each SOD.

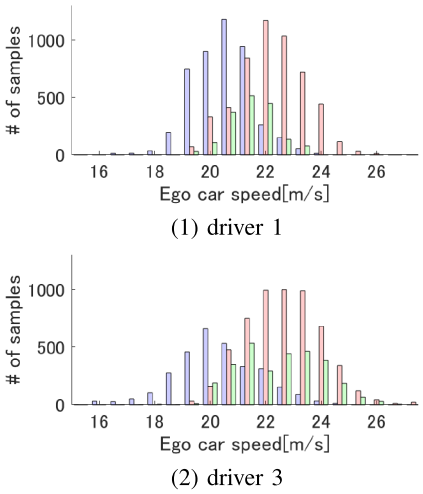

Fig. 8. Distribution of speed v^E in each SOD.

$j = 3$ pays substantial attention to $d^{M,E}$ in both switching from *UNDECIDED* to *ACCEPT* and *REJECT*. Note that the significance of each regressor variable for decision-making varies from driver to driver.

The distribution of $d^{L,E}$, that is, the relative distance between Car E and Car L, and v^E, that is, the driving speed of Car E, of drivers 1 and 3 are depicted in Fig.7 and Fig.8, respectively. In Fig.7-(1), a clear difference in the distribution of $d^{L,E}$ can be observed among the decision states for driver 1. Normally, $d^{L,E}$ becomes shorter than the other states when SOD is *REJECT* to show the intention to a merging car. Moreover, the histograms of the relative distance of driver 3 in *ACCEPT* and *UNDECIDED* are similar. This implies that driver 3 does not change the following distance irrespective of whether he accepts or not. The parameters $\theta = (d_{\mathrm{ref}}(1), \theta = d_{\mathrm{ref}}(2), and \theta = d_{\mathrm{ref}}(3))^T$ to follow Car L is determined by obtaining the average of $d^{L,E}$ in each state, as discussed in section II-C. The driving speed has a clear difference between the *ACCEPT* and *REJECT* states of both drivers 1 and 3 in Fig.8. Both drivers 1 and 3 accelerate, preventing Car M from merging into the front of Car E in the

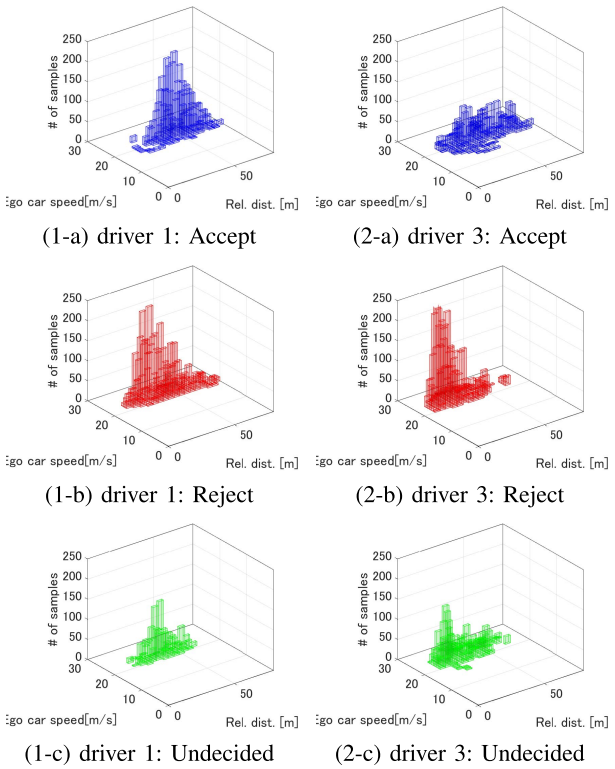

(1-a) driver 1: Accept (2-a) driver 3: Accept

(1-b) driver 1: Reject (2-b) driver 3: Reject

(1-c) driver 1: Undecided (2-c) driver 3: Undecided

Fig. 9. 2D distribution of the distance and driving speed in each SOD.

REJECT state, and decelerate in the *ACCEPT* state to secure additional margin. In Fig.9, two-dimensional (2D) histograms of the relative distance and driving speed of drivers 1 and 3 in each SOD (*ACCEPT* , *REJECT* and *UNDECIDED*) are presented. Although the data distribution of drivers 1 and 3 is similar in *UNDECIDED* , a large difference can be observed in the *ACCEPT* and *REJECT* states. Driver 3 can be considered as a more aggressive driver than driver 1 because the former takes shorter distance and higher speed in the *REJECT* state.

An important advantage of the driving behavior modeling by separating the decision-making and motion control parts is the understandability of the model. This is more emphasized when we are required to develop a driver model for a complex environment. Although a considerably complex model, such as a deep neural network, sometimes provides high estimation performance, realizing a clear meaning of the obtained model is often not easy. This condition will be a negative factor to be exploited for the design of the control strategy discussed in a later section.

F. Verification of the Identified Model

The model of the decision-making part is again focused and verified in this section. SOD is estimated using the identified logistic regression model and the estimation accuracy is tested with a cross-validation method. The five-fold cross-validation method is applied to verify the estimation performance of SOD. Each driver model obtained from each driver's measurement is tested independently.

Figure 10 shows the technique of evaluating the correctness of the estimated SOD. The red dashed line indicates one

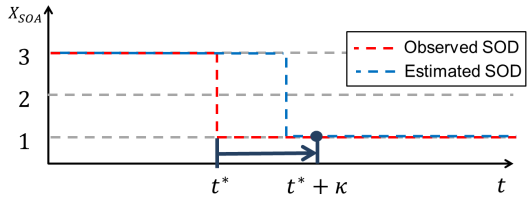

Fig. 10. Evaluation of model estimation.

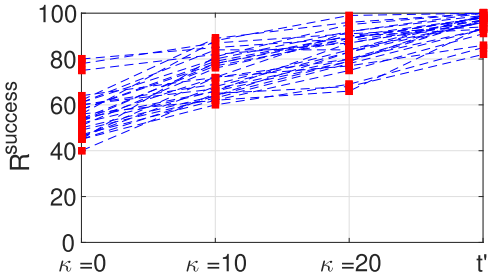

Fig. 11. Success ratio of the merging acceptance state estimation.

of profiles of the observed SOD in the experiment, which is introduced in section II-D. The blue dashed line denotes the profile of the estimated SOD using the identified logistic regression model in section II-E. Furthermore, t^* is the time when SOD is switched from *UNDECIDED* to the other states, i.e., the time when either the *ACCEPT* or *REJECT* button on the steering wheel is pushed. This time is assumed as the time instance in this study when the driver has made the decision. Given that the accuracy of the model cannot be perfect, the estimated profile of SOD may have an estimation error or delay. A trial is regarded as successful if the SOD estimated by the model matches the observed one after κ [steps] from t^*. The success rates, $\mathbf{R}^{success}(\kappa)$, are calculated by counting the successful trials among the 100 trials for the given κ. That is, the success rate $\mathbf{R}^{success}(\kappa)$ evaluates the rate of the trials wherein the obtained model can estimate the measured SOD by using the identified model until κ steps after the driver's decision-making process.

Figure 11 shows the result of the success rate at $\kappa = 0$, $\kappa = 10$, and $\kappa = 20$ steps (equivalent to 0, 1, and 2 s, respectively) and at t' (the time when Car E reaches p_β). Note that the duration from t^* to t' differs in each trial because the decision-making time t^* and the driving speed of these cars vary. Generally, the estimated probability of the SOD tends to converge to *ACCEPT* or *REJECT* as Car E approaches the end of the merging lane, as denoted by p_γ in Fig.1. Therefore, $\mathbf{R}^{success}$ normally increases with κ. The average of the resulting success rate at time t' is 95.5%. This result indicates that the proposed model can estimate the SOD, i.e., whether Car E allows the merging of Car M or not with 95.5% accuracy before Car E reaches the start point of the acceleration area, p_β.

The result shows the practical accuracy despite the simple structure of the model. However, potential improvement can be achieved on its accuracy.

Two strategies are used to improve the constructed model. The first idea to improve the model is changing the model structure and adding additional explanatory variables that may

affect the driver's decision-making and driving speed. For example, some conditions of the driver, such as rushing, drowsiness, and fatigue, may influence his driving. Several studies have attempted to capture this type of driver state [35] in real time. These states can be candidates of additional explanatory variables once they are measured. In addition, other cars that are not involved in the model, such as cars in front of Car L, behind of Car E, and in front and/or behind of Car M , may have an effect on both decision-making and speed control of the drivers of Car M and Car E . To include these factors, further experiments and measurements with an appropriate task setting are necessary.

The second idea to improve the accuracy of the model is considering slow changes in the parameters. The driving behavior changes gradually during driving depending on the driver's fatigue and driving experiences. To address these slow changes, the identified model can be adapted online by updating these parameters gradually by using a real-time system identification technique [25]. However, further studies are necessary for these accuracy improvements in the future.

In this study, the average driver model will be used for prediction in the MPC in a later section. However, the prediction performance of MPC can also be improved if a highly specific driver model is available, which is characterized by classifying the obtained models based on the driving tendency, such as aggressive and conservative. By using the representative driver model for each class of driving tendency in this case, the control performance of MPC will be improved. In addition, recognition of the driving tendency of the surrounding cars is easier than estimating the individual model parameters in real time.

III. Formulation of the Merging Behavior Control Based on Decision Entropy

A. Overview of the Proposed Control Scheme

This section proposes a novel control method for merging behavior using the obtained driver model of the car on the main lane. The proposed control method considers not only the motion of the cars on the main lane but also their decision-making characteristics, i.e., SOD. This algorithm is supposed to be implemented on the merging car (i.e., Car M).

The proposed control scheme comprises a two-stage speed control of the merging car. The first one is to achieve a fast consensus with the cars on the main lane by optimizing the speed (consensus control). The key idea in this stage is to minimize the entropy of the SOD of the drivers on the main lane by optimizing the speed of the merging vehicle. By exploiting this idea in the MPC framework, the decision-making vagueness of the drivers on the main lane is reduced. This scheme is quantitatively formulated using the identified decision model and realized by adopting the RMPC approach. The second one is to finalize the merging task after achieving a consensus in the first stage (merging control). Owing to the consensus mechanism at the first stage, the control difficulty in the second stage is minimized.

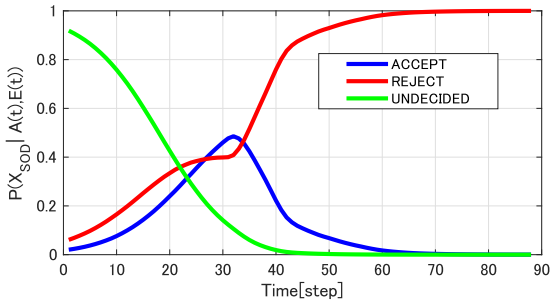

Fig. 12. Example of high-entropy case.

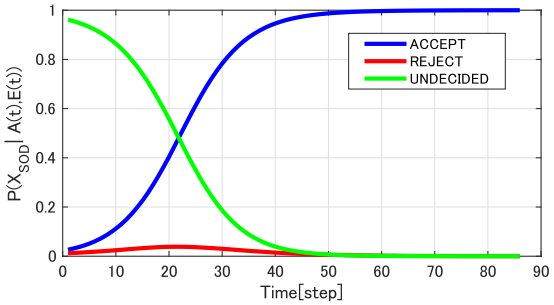

Fig. 13. Example of low-entropy case.

B. Decision Entropy of Acceptance

A novel quantitative index, "decision entropy," is introduced to evaluate the vagueness of the SOD of the driver. The decision entropy, $S^c(t)$, at time t is defined using a decision model as follows:

$$S^c(t) = -\sum_{s=1}^{3} P_s^c(t) \times \log_2 P_s^c(t), \tag{13}$$

$$P_s^c(t) = P(X_D^C(t) = s \mid \phi^c(t), \mathbf{M}^{j(c)}), \tag{14}$$

where c is the index of the car on the main lane and the function $j(c)$ returns the index of the driver model assigned to Car c . Furthermore, $X_D^C(t)$ and $\phi^c(t)$ are the SOD and regressor vector of Car C at time t, respectively. $P_s^j(t)$ is the probability that the SOD utilizes a state of s at time t with the driver model j. This decision entropy, $S^c(t)$, uses a smaller value if the probability of all states is close to 0 or 1.

The sample profiles of SOD probability in the case of high and low entropies are depicted in Figs.12 and 13, respectively. These profiles are calculated using the observed driving data. As shown in Fig.12, both *ACCEPT* and *REJECT* probabilities are increasing before $t = 35$ s. This implies that the decision-making of the driver is not completed before $t = 35$ s; hence, the decision entropy employs a large value in this duration. Meanwhile, the profiles of SOD probability shown in Fig.13 converge faster to 0 or 1 than that in Fig.12. Thus, the decision entropy utilizes a smaller value in a short time duration than the case in Fig.12. This implies that the driver in this case can make a decision more easily than that in the high-entropy case.

C. Formulation of Consensus Control

The consensus control is designed for Car M to optimize its approaching speed by minimizing the decision entropy of

e drivers on the main lane. The MPC framework is used as a basic control scheme. MPC is known as a promising control strategy that can optimize a specified cost function by considering the physical constraint and dynamical model of the target system in real time.

The total decision entropy of all drivers on the main lane over a certain finite horizon is regarded as the cost function. Hence, the proposed control scheme is assumed to render the decision-making of drivers on the main lane easy by reducing the vagueness of the decision. To achieve this objective, the MPC-based consensus control is formulated as follows.

given:

$$x(0|t) = x(t),\ L_w, \qquad (t \in \{1, 2, \cdots, T\}) \tag{15}$$

find:

$$u^M(k|t) \qquad (k \in \{1, 2, \cdots, K\} \tag{16}$$

which minimize:

$$J_{cons}(t) = \sum_{k=1}^{K} \sum_{c=1}^{N} S^c(k|t)$$

$$S^c(k|t) = -\sum_{s=1}^{3} P(X^c_{SOD}(k|t) = s|\phi^c(k|t), \mathbf{M}^{j(c)}) \tag{17}$$

$$\times \log_2 P(X^c_{SOD}(k|t) = s|\phi^c(k|t), \mathbf{M}^{j(c)}) \tag{18}$$

subject to:

$$u_{MIN} \leqq u^M(k|t) \leqq u_{MAX} \tag{19}$$

$$p^c(k+1|t) = p^c(k|t) + v^c(k|t)\Delta t \quad \text{for } {}^\forall c \in \{0, \cdots, N\} \tag{20}$$

$$v^c(k+1|t) = v^c(k|t) + a^c(k|t)\Delta t \quad \text{for } {}^\forall c \in \{0, \cdots, N\} \tag{21}$$

$$a^c(k|t) = f(\mathbf{M}^{j(c)}, \phi^c(k|t)) \quad \text{for } {}^\forall c \in \{1, \cdots, N\} \tag{22}$$

$$a^0(k|t) = 0, \tag{23}$$

$$THW_F(j|t) = (p^F(j|t) - p^M(j|t))/v^M(j|t) > THW^{th} \quad \text{for } {}^\forall j \in \{j \mid p_\gamma - 50 < p^M(j|t) < p_\gamma\} \tag{24}$$

Here, t is the current time and k is the time index in the prediction horizon. In addition, K is the total number of steps in the prediction horizon (i.e., length of horizon) and N is number of cars driving on the main lane except Car 0 . The state of first step in the prediction horizon, $x(0|t) = [p^0(0); v^0(0); p^1(0); v^1(0); \cdots; p^N(0); v^N(0)]$, comprises the position and speed of cars on the main lane observed at time t. The input $u_M(t)$ (driving speed of Car M) is limited between $u_{MIN} = 16.67$ m/s and $u_{MAX} = 33.33$ m/s. The time headway, THW^{th}, is also restricted to be higher than THW^{th} (set to 0.5 s in this study) for the closest leading vehicle on the main lane (Car c-1). Meanwhile, the acceleration of Car c in (22) is calculated from the motion control model defined in section II-C. The cost function $J_{cons}(t)$ evaluates the total decision entropy of cars from Car 1 to Car N over the prediction horizon.

D. Merging Control

After realizing consensus with the drivers on the main lane, the merging task is finalized by executing the merging control. The most important requirement for this second stage control is safety. Although the control objective is changed from the first stage (consensus control), similar MPC-based control is used for merging control. Only the cost function is modified after the consensus is made.

The condition to determine whether a consensus was made is defined as follows:

$$[P^B(X_{SOD}(t)=1) > p_{th}] \wedge [P^F(X_{SOD}(t)=2) > p_{th}], \tag{25}$$

where $P^B(X_{SOD}(t))$ and $P^F(X_{SOD}(t))$ represent the estimated probability that the closest behind vehicle (Car B) on main lane accepts the Car M and the closest frontal vehicle (Car F) on main lane rejects the Car M , respectively. Threshold p_{th} in this study is set to 0.9.

The cost function used for merging control is expressed as follows:

$$J_{merg}(t) = w_1 \|d_{\text{ref}} - d^{F,M}(1|t)\|_1 + w_2 \|v^{F,M}(1|t)\|_1, \tag{26}$$

where $d_{\text{ref}} (= 25\text{m})$ is the reference distance, and $d^{F,M}(1|t)$ and $v^{F,M}(1|t)$ are The longitudinal distance and relative speed between Car M and Car F at time t and step $k = 1$ in the prediction horizon, respectively. Furthermore, $\| \cdot \|_1$ is 1-norm (i.e., absolute value). The weight parameters w_1 and w_2 are determined by trial and error. This cost function mainly focuses on driving safety to finalize the merging task.

Although various control methods for merging have been suggested, we adopt the previous MPC-based idea to be consistent with the consensus control. This leads to the advantage of the proposed strategy for the implementation.

For the lateral motion, a remarkably simple lateral controller for Car M is introduced as follows:

$$u_y^M(t) = \begin{cases} -0.05, & \text{if}[p_\beta < p^M(t)] \wedge [d^{M,B} > d_{\text{ref}}] \\ & \quad \wedge [d^{F,M} > d_{\text{ref}}] \\ 0, & \text{otherwise,} \end{cases} \tag{27}$$

where u_y^M is the lateral speed and the reference distance d_{ref} is set to 25m.

E. Implementation of MPC Using a Randomized Approach

The proposed MPC problems in section III-C and section III-D include nonlinear cost function and constraints. Hence, a nonlinear optimization solver, which sometimes leads to undesirable computational complexity and time, must be applied. To overcome this difficulty, RMPC [26]–[28] is introduced to compute a semi-optimal solution. Recently, RMPC has attracted attention as a promising strategy for stochastic MPC and/or nonlinear MPC problems [30].

The basic idea of RMPC is based on random input sampling similar to the Monte Carlo method and forward calculation of state prediction. The cost function is computed for each input sample and the best sample is adopted as the suboptimal input.

Similar to the standard MPC scheme, the optimization of the input over a finite prediction horizon is executed every

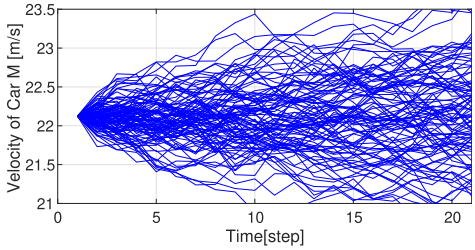

Fig. 14. Example profiles of sampled input series ($N_s = 100$).

TABLE V
PARAMETERS IN VALIDATION

Δt	0.1 s
K	20
N_s	500
L_w	300

$v^M(0)$	22.22 m/s
$p^0(0), v^0(0)$	1050 [m], 22.22 m/s
$p^M(0)$	$[p^3(0)-30,\ p^3(0)+30]$
$w_1,\ w_2$	20, 1

control cycle. The first step of RMPC is to generate samples of the input series, $u^M(k|t)$ over $\forall k \in \{1, 2, \cdots, K\}$ at time t. These are generated according to the following uniform distribution.

$$P(\Delta u^M(k|t)) = \begin{cases} 1/2h, & \text{if } \Delta u^M(k|t) \in (-h, h), \\ 0, & \text{otherwise,} \end{cases} \tag{28}$$

Here, $\Delta u^M(k|t) = u^M(k+1|t) - u^M(k|t)$ is the time difference of the control input (speed of Car M) over one control cycle (0.1 s), h is the value range of $\Delta u^M(k|t)$, and $h = 0.98 \times \Delta t$ is used in this study. This is decided by considering the time constant of the dynamics of the car. The input series is referred to as a random walk process. Examples of the generated input series with the number of samples $N_s = 100$ are shown in Fig.14. Importantly, this distribution should be determined to cover the input and state space to find the "optimal" solution.

An input series that employs the minimum value in the cost function is used as a suboptimal solution, and the first step signal in the series is applied to Car M (similar to the standard MPC). Discussions on the number of required samples for assurance of quality of the solution are available [31]. According to the discussion in [31], $N_s \simeq 458$ is obtained for the proposed RMPC by setting the level to $\alpha = 0.01$ and confidence $1-\sigma$, where $\sigma = 0.01$. Therefore, N_s is set to 500 in the experiments.

IV. VERIFICATION THROUGH NUMERICAL EXPERIMENTS

A. Simulation Setting

Numerical experiments are performed to verify the usefulness of the proposed merging behavior control. The target situation is shown in Fig.1.

We assume that Car M and the cars on the main lane cannot see each other before reaching p_α ($x^M(t) = 1000$), where $x^M(t)$ is the longitudinal position of Car M.

Car M, whose position is between p_α and p_β ($x^M(t) = 1000$–1300), is noticeable from the cars on the main lane (Car 1 –Car N) and from Car M, and vice versa. The accelerating lane begins from point p_β ($x = 1300$) and ends at point p_γ ($x = 1500$). Car 0, the leading car of the car fleet, runs with a constant speed of $v_0 = 22.22$ m/s. The behaviors of Car 1 ,$\cdots$, Car 5 are simulated using the identified driver model obtained in section II. Various driver models are randomly assigned to the cars from all 28 obtained driver models, $\mathbf{M}^j$ ($j = \{1, \cdots, 28\}$). $k_d = 0.001$ and $k_p = 0.005$ are used for (8) in these driver models.

TABLE VI
PARAMETERS OF THE AVERAGE MODEL $\mathbf{M}^{\text{ave}}$

average	const.	$d^{M,E}$	$v^{M,E}$	$a^{M,E}$	$d^{L,E}$	$d^{\gamma,E}$	L_w
η_1	-0.11	3.25	0.47	0.49	0.22	-1.38	0.42
η_2	-0.27	-0.84	-0.29	-0.18	-0.54	-1.59	0.63

average	$d_{\text{ref}}(1)$	$d_{\text{ref}}(2)$	$d_{\text{ref}}(3)$
θ	54.8	39.4	40.3

One of the critical issues for the design of merging control is the availability of communication among the cars. Regarding the current technological situation of the vehicle, an automated car is required to consider the behavior of the car driven manually without any communication capability. Therefore, we assume that Car M can obtain relative information to the cars on the main lane by using implementable sensors but cannot know which driver model is assigned to Car 1 to Car 5 in the simulation. Instead of using the individual model to predict the driving behavior of Car 1 –Car 5, an average model $\mathbf{M}^{\text{ave}}$, which is identified using all participants' driving data, is used for MPC.

The parameters of the average model are listed in Table VI. However, note that the identified reference distances, $d_{\text{ref}}(i)$, are not directly used. This is because the reference distances, which highly depend on the preference of the driver on the main lane, are sometimes predictable by sensing their behavior without any communication. Thus, these parameters are calculated using the following equation to improve the prediction performance of the behavior of cars in the main lane.

$$d^i_{\text{ref}}(s) = \begin{cases} d^{i-1,i}(0), & \text{if } s = 1, \\ (54.8/40.3) \times d^{i-1,i}(0), & \text{if } s = 2, \\ (39.4/40.3) \times d^{i-1,i}(0), & \text{if } s = 3, \\ \forall i \in \{1, 2, \cdots, 5\} \end{cases} \tag{29}$$

This adaptation is in accordance with the idea that the reference distances $d^i_{\text{ref}}(1)$ and $d^i_{\text{ref}}(2)$ for Car$i$ are proportionally adjusted on the basis of the initial observation of the distance between the target car and the car in front of it.

The initial distance between Car$i$ and Car$i-1$ for $i \in \{1, 2, \cdots, 5\}$ is set to $d^i_{\text{ref}}(3)$ of the driver model $\mathbf{M}^j(i)$, which is assigned to each car at the start of the simulation. The initial position of Car M is randomly determined from the uniform distribution with the range of $[p_3(0)-30,\ p_3(0)+30]$, as listed in Table V. Other parameters used in the simulations are also listed in Table V. The numerical experiments are performed 10,000 times by changing the initial position of Car M and driver model assignment for the cars on the main lane.

B. Simulation Results

Figure 15 shows one of the resulting profiles of the positions of all considered cars. The driver models,

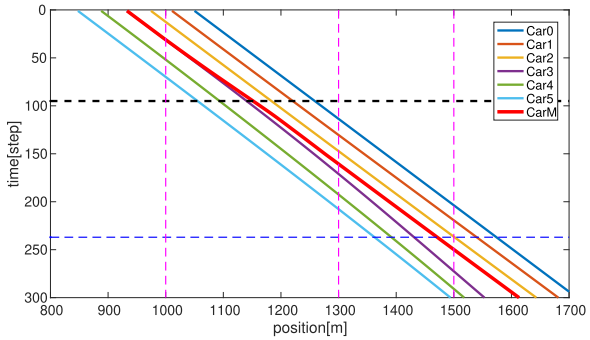

Fig. 15. Resulting profiles of the vehicle's position.

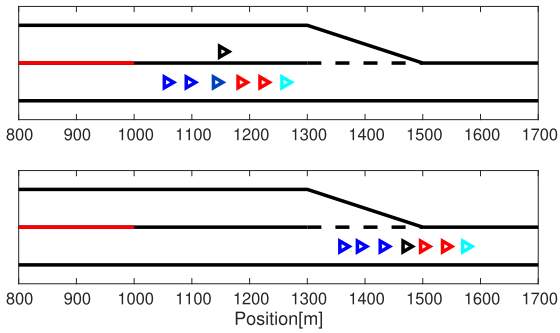

Fig. 16. View of the simulation at $t = 95$ step (top) and $t = 237$ step (bottom).

$[\mathbf{M}^{25}, \mathbf{M}^{11}, \mathbf{M}^{16}, \mathbf{M}^{15}, \mathbf{M}^{12}]$ are assigned to Car 1 –Car 5 in this simulation. The initial position of Car M is set to $p_3(0) + 0.2$. Meanwhile, the horizontal and vertical axes represent the position and time, respectively.

Here, a "completion time of consensus," t^{cons}, is defined to evaluate the time required to complete the consensus making. t^{cons} is defined as the time when the SOD of Car F and Car B estimated by Car M (using the average model) agree with the SOD computed using the independent driver models assigned to Car F and Car B . t^{cons} is the minimum value of $\tau \in \{1, 2, \cdots, T\}$ that satisfies

$$\Big[[\bar{X}_D^B(\tau \mid \mathbf{M}^{\text{ave}}) = \bar{X}_D^B(\tau \mid \mathbf{M}^{j(B)})] \wedge [\bar{X}_D^B(\tau \mid \mathbf{M}^{\text{ave}}) \neq 3]\Big]$$
$$\wedge \Big[[\bar{X}_D^F(\tau \mid \mathbf{M}^{\text{ave}}) = \bar{X}_D^F(\tau \mid \mathbf{M}^{j(F)})] \wedge [\bar{X}_D^F(\tau \mid \mathbf{M}^{\text{ave}}) \neq 3]\Big]$$
$$\bar{X}_D^c(\tau \mid \mathbf{M}^j) = \begin{cases} 1 & \text{if } P(X_D^c(t) = 1 \mid \phi^c(t), \mathbf{M}^j) > p_{th} \\ 2 & \text{if } P(X_D^c(t) = 2 \mid \phi^c(t), \mathbf{M}^j) > p_{th} \\ 3 & \text{otherwise} \end{cases}$$
$$^{\forall}c \in \{F, B\}. \qquad (30)$$

Here, T is the number of simulation steps and $\bar{X}_D^c(\tau \mid \mathbf{M}^j)$ denotes the estimated SOD of Car F or Car B using the driver model $\mathbf{M}^j$ (either driver model assigned to Car F and Car B or average model) under a specified threshold on the probability. Then, $\bar{X}_D^B(\tau \mid \mathbf{M}^{ave})$ represents the estimated SOD of Car B using the average model (used in MPC) and $\bar{X}_D^B(\tau \mid \mathbf{M}^{j(B)})$ indicates the estimated SOD of Car B using a driver model assigned to Car B . Note that the latter is used only for verification and is not available for MPC.

In Fig.15, the black dashed line shows the completion time of the consensus control, t^{cons}, in case of $p_{th} = 0.9$ ($t^{cons} =$ 95 step), and blue dashed line shows the time to finalize the merging into the main lane ($t = 237$ step). The vertical purple dashed lines represent the points p_α, p_β, and p_γ. Figure 16 shows the top views of the car positions at time steps $t = 95$ and 237. Here, triangles indicate the cars and red and blue colors represent the computed SOD of the cars on the main lane (blue: *ACCEPT*, red:*REJECT*). In this example, the cars achieve consensus when Car M passes 150 m ahead of the start position of the acceleration area.

The proposed merging behavior control is compared with the constant speed control to verify the usefulness of the former. In the constant speed control, the speed of Car M is set to $v_M = 22.22$[m/s] during its entire merging task.

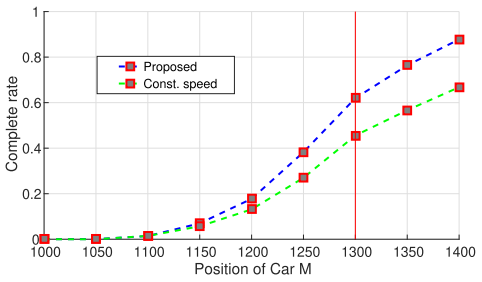

Fig. 17. Resulting consensus completion rate ($p_{th} = 0.9$).

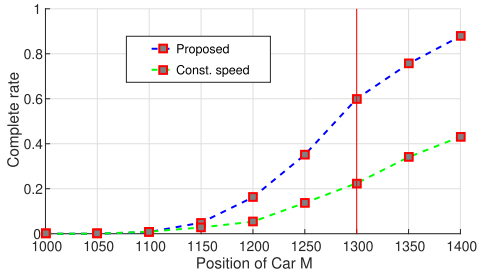

Fig. 18. Resulting consensus completion rate in initial difficult condition ($p_{th} = 0.9$).

The relation between the consensus completion rate (CCR) and position of Car M is depicted in Fig.17 under the threshold $p_{th} = 0.9$. CCR is defined as the ratio of the number of simulation trials that realize consensus before Car M passes the position x in all simulation trials. The blue and green dashed lines represent the profiles of CCR of the proposed merging behavior control and constant speed control, respectively. As the position of Car M advances to the end of the acceleration area, the CCRs of both methods, as well as the difference between them, increase. The proposed control provides 18.1 point higher than the constant speed control in the CCR at point $x = 1300$ m, that is, the start point of the acceleration area. In case of the proposed merging behavior control, Car M completes the merging into the main lane at an average of approximately $x = 1400$, and 86.9% of all simulation trials achieve consensus with cars on the main lane before passing $x = 1400$.

Finally, a considerably difficult situation is tested with a limited number of trials. The sampling range for the initial position of Car M is changed to $[p_3(0) - 10,\ p_3(0) + 10]$ in this simulation. The resulting CCR is shown in Fig.18.

Considering that Car M starts from a closer position to the car driving on the main lane (in this case, Car 3), achieving a consensus between Car M and Car 3 becomes difficult. Consequently, the CCR with constant speed control indicates much lower values than the previous case. However, we confirm that the proposed merging behavior control can maintain a high CCR even in a difficult situation. Hence, we assume that the proposed control can reduce the decision-making burden of the drivers on the main lane.

V. Conclusion

In this study, the decision-making characteristics of the driver on the main lane, whether he accepts a merging car or not at a highway junction, were modeled and the application of the model to the design of merging behavior control was proposed. First, the driving behavior on the main lane at the highway junction was observed using a DS. Particularly, the driver's acceptance for a merging car coming from the merging lane was focused in the measurement. The measured driver's state of acceptance was quantitatively modeled using a logistic regression model, and then, the prediction performance of the identified model was verified. Second, a design scheme of the merging behavior control of the car on the merging lane was proposed, which comprised a two-stage control, namely consensus control and merging control. Both control schemes were realized using the RMPC framework. The consensus control used the entropy of the state of acceptance of the driver on the main lane as the cost function. Owing to this control, a considerate merging behavior was realized. The results of the numerical experiments demonstrate that the proposed control scheme has a high contribution potential to the implementation of an automated vehicle in an actual traffic environment.

References

[1] A. Calvi and M. R. De Blasiis, "Driver behavior on acceleration lanes: Driving simulator study," *Transp. Res. Rec.*, vol. 2248, no. 1, pp. 96–103, 2011.

[2] J. Zhou, J. Fang, and R. Zhou, "Study on the safety length of acceleration and deceleration lane of left-side ramp on freeway," in *Proc. 16th Int. Conf. Road Saf. Four Continents*, 2013, pp. 1–11.

[3] S. E. Shladover, "Operation of merge junctions in a dynamically entrained automated guideway transit system," *Transp. Res. A, Gen.*, vol. 14, no. 2, pp. 85–112, 1980.

[4] V. Kanagaraj, K. Srinivasan, and R. Sivanandan, "Modeling vehicular merging behavior under heterogeneous traffic conditions," *Transp. Res. Rec.*, vol. 2188, no. 1, pp. 140–147, 2010.

[5] M. Sarvi, M. Kuwahara, and A. Ceder, "Freeway ramp merging phenomena in congested traffic using simulation combined with a driving simulator," *Comput.-Aided Civil Infrastruct. Eng.*, vol. 19, no. 5, pp. 351–363, 2004.

[6] M. Sarvi and M. Kuwahara, "Microsimulation of freeway ramp merging processes under congested traffic conditions," *IEEE Trans. Intell. Transp. Syst.*, vol. 8, no. 3, pp. 470–479, Sep. 2007.

[7] J. Al-Obaedi and S. Yousif, "Microsimulation model for motorway merges with ramp-metering controls," *IEEE Trans. Intell. Transp. Syst.*, vol. 13, no. 1, pp. 296–306, Mar. 2012.

[8] H. Guzmán, M. Lárraga, L. Alvarez-Icaza, and F. Huerta, "On-ramp traffic merging modeling based on cellular automata," in *Proc. IEEE Eur. Modelling Symp. (EMS)*, Oct. 2015, pp. 103–109.

[9] J. Rios-Torres and A. A. Malikopoulos, "Automated and cooperative vehicle merging at highway on-ramps," *IEEE Trans. Intell. Transp. Syst.*, vol. 18, no. 4, pp. 780–789, Apr. 2017.

[10] V. Milanés, J. Godoy, J. Villagra, and J. Perez, "Automated on-ramp merging system for congested traffic situations," *IEEE Trans. Intell. Transp. Syst.*, vol. 12, no. 2, pp. 500–508, Jun. 2011.

[11] X. Lu, H.-S. Tan, S. E. Shladover, and J. K. Hedrick, "Implementation of longitudinal control algorithm for vehicle merging," in *Proc. 5th Int. Symp. Adv. Vehicle Control*, 2000, pp. 1–8.

[12] A. Mosebach, S. Röchner, and J. Lunze, "Merging control of cooperative vehicles," *IFAC-PapersOnLine*, vol. 49, no. 11, pp. 168–174, 2016.

[13] W. Cao, M. Muka, T. Kawabe, H. Nishira, and N. Fujiki, "Merging trajectory generation for vehicle on a motor way using receding horizon control framework consideration of its applications," in *Proc. IEEE Conf. Control Appl. (CCA)*, 2014, pp. 2127–2134.

[14] M. Mukai, H. Natori, and M. Fujita, "Model predictive control with a mixed integer programming for merging path generation on motor way," in *Proc. IEEE Conf. Control Technol. Appl. (CCTA)*, Aug. 2017, pp. 2214–2219.

[15] D. Marinescu, J. Čurn, M. Bouroche, and V. Cahill, "On-ramp traffic merging using cooperative intelligent vehicles: A slot-based approach," in *Proc. 15th Int. IEEE Conf. Intell. Transp. Syst.*, Sep. 2012, pp. 900–906.

[16] T. Awal, L. Kulik, and K. Ramamohanrao, "Optimal traffic merging strategy for communication-and sensor-enabled vehicles," in *Proc. 16th Int. IEEE Conf. Intell. Transp. Syst.*, Oct. 2013, pp. 1468–1474.

[17] M. Papageorgiou, I. Papamichail, A. D. Spiliopoulou, and A. F. Lentzakis, "Real-time merging traffic control with applications to toll plaza and work zone management," *Transp. Res. C, Emerg. Technol.*, vol. 16, no. 5, pp. 535–553, 2008.

[18] L. Li and D. Zhang, "Spatial characteristics of merging decision making and implementation at highway work zone," in *Proc. 4th Int. Conf. Transp. Inf. Saf. (ICTIS)*, Aug. 2017, pp. 1081–1087.

[19] C. Dong, J. M. Dolan, and B. Litkouhi, "Intention estimation for ramp merging control in autonomous driving," in *Proc. IEEE Intell. Vehicles Symp. (IV)*, Jun. 2017, pp. 1584–1589.

[20] K. A. Semprun, P. C. Y. Chen, W. Chen, and Z. Zhao, "The concept of stimuli-induced equilibrium point and its application in ramp-merging control," *IEEE Trans. Intell. Transp. Syst.*, vol. 19, no. 9, pp. 2814–2825, Sep. 2018, doi: 10.1109/TITS.2017.2761865.

[21] S. Ueda and T. Wada, "Modeling of drivers' decision making of merging space on expressways," in *Proc. 41st Annu. Conf. IEEE Ind. Electron. Soc.*, Nov. 2015, pp. 637–642.

[22] H. Okuda, K. Harada, T. Suzuki, S. Saigo, and S. Inoue, "Modeling and analysis of acceptability for merging vehicle at highway junction," in *Proc. IEEE 19th Int. Conf. Intell. Transp. Syst. (ITSC)*, Nov. 2016, pp. 1004–1009.

[23] H. Okuda, K. Harada, T. Suzuki, S. Saigo, and S. Inoue, "Design of automated merging control by minimizing decision entropy of drivers on main lane," in *Proc. IEEE Intell. Vehicles Symp. (IV)*, Jun. 2017, pp. 640–646.

[24] T. Suzuki, S. Yamada, S. Hayakawa, N. Tsuchida, T. Tsuda, and H. Fujinami, "Modeling of drivers collision avoidance behavior based on hybrid system model: An approach with data clustering," in *Proc. IEEE Int. Conf. Syst., Man Cybern.*, vol. 4, Oct. 2005, pp. 3817–3822.

[25] H. Okuda, N. Ikami, T. Suzuki, Y. Tazaki, and K. Takeda, "Modeling and analysis of driving behavior based on a probability-weighted ARX model," *IEEE Trans. Intell. Transp. Syst.*, vol. 14, no. 1, pp. 98–112, Mar. 2013.

[26] J. L. Piovesan and H. G. Tanner, "Randomized model predictive control for robot navigation," in *Proc. IEEE Int. Conf. Robot. Automat.*, May 2009, pp. 94–99.

[27] G. Schildbach, G. C. Calafiore, L. Fagiano, and M. Morari, "Randomized model predictive control for stochastic linear systems," in *Proc. Amer. Control Conf. (ACC)*, 2012, pp. 417–422.

[28] M. Vidyasagar, "Randomized algorithms for robust controller synthesis using statistical learning theory," *Automatica*, vol. 37, no. 10, pp. 1515–1528, 2001.

[29] D. D. Dunlap, E. G. Collins, Jr., and C. V. Caldwell, "Sampling based model predictive control with application to autonomous vehicle guidance," in *Proc. Florida Conf. Recent Adv. Robot.*, 2008, pp. 1–6.

[30] G. Ripaccioli, D. Bernardini, S. Di Cairano, A. Bemporad, and I. V. Kolmanovsky, "A stochastic model predictive control approach for series hybrid electric vehicle power management," in *Proc. Amer. Control Conf.*, Jun./Jul. 2010, pp. 5844–5849.

[31] X. Zhang, S. Grammatico, G. Schildbach, P. Goulart, and J. Lygeros, "On the sample size of random convex programs with structured dependence on the uncertainty," *Automatica*, vol. 60, pp. 182–188, Oct. 2015.

[32] H. Jia, Y. Tan, and L. Yang, "Modeling vehicle merging behavior in urban expressway merging sections based on logistic model," in *Proc. Int. Conf. Transp., Mech., Elect. Eng. (TMEE)*, 2011, pp. 656–659.

[33] J. B. Rawlings, D. Q. Mayne, and M. M. Diehl, *Model Predictive Control: Theory, Computation, and Design*, 2nd ed. San Francisco, CA, USA: Nob Hill, 2017.
[34] J. McCall and M. M. Trivedi, "Video-based lane estimation and tracking for driver assistance: Survey, system, and evaluation," *IEEE Trans. Intell. Transp. Syst.*, vol. 7, no. 1, pp. 20–37, Mar. 2006.
[35] L. Li, D. Wen, N.-N. Zheng, and L.-C. Shen, "Cognitive cars: A new frontier for ADAS research," *IEEE Trans. Intell. Transp. Syst.*, vol. 13, no. 1, pp. 395–407, Mar. 2012.

Hiroyuki Okuda (M'17) was born in Gifu, Japan, in 1982. He received the B.E. and M.E. degrees in advanced science and technology from the Toyota Technological Institute, Japan, in 2005 and 2007, respectively, and the Ph.D. degree in mechanical science and engineering from Nagoya University, Japan, in 2010. He was a PD Researcher at CREST, JST, from 2010 to 2012, and also an Assistant Professor at the Green Mobility Collaborative Research Center, Nagoya University, from 2012 to 2016. He was a Visiting Researcher of the Mechanical Engineering Department, UC Berkeley, in 2018. He is currently an Assistant Professor with the Department of Mechanical Science and Engineering, Nagoya University. His research interests are in the areas of system identification of hybrid dynamical system and its application to the modeling and the analysis of human behavior, and the human-centered system design of autonomous/human-machine cooperative system. He is a member of the IEEJ, SICE, JSAE, and JSME.

Tatsuya Suzuki (M'91) was born in Aichi, Japan, in 1964. He received the B.S., M.S., and Ph.D. degrees in electronic mechanical engineering from Nagoya University, Japan, in 1986, 1988, and 1991, respectively. From 1998 to 1999, he was a Visiting Researcher of the Mechanical Engineering Department, UC Berkeley. He is currently a Professor with the Department of Mechanical Systems Engineering, and the Executive Director of the Global Research Institute for Mobolity in Society (GREMO), Nagoya University. He has also been a Principal Investigator with JST, CREST, from 2013 to 2019. His current research interests are in the areas of analysis and design of human-centric intelligent mobility systems, and integrated design of transportation and smart grid systems. He is a member of the SICE, ISCIE, IEICE, JSAE, RSJ, JSME, and IEEJ. He won the Best Paper Award at the International Conference on Autonomic and Autonomous Systems 2017 and the Outstanding Paper Award at the International Conference on Control Automation and Systems 2008. He also won the Journal Paper Award from the IEEJ, SICE, and JSAE, in 1995, 2009, and 2010, respectively.

Kota Harada was born in Aichi, Japan, in 1994. He received the B.S. degree in electronic mechanical engineering from Nagoya University, Japan, in 2016. His research interests are in the areas of modeling driver decision characteristics and its application to vehicle control.

Shintaro Saigo was born in Kanagawa, Japan, in 1986. He received the B.S., M.S., and Ph.D. degrees in mechanical systems engineering from the Tokyo University of Agriculture and Technology, Japan, in 2009, 2011, and 2014, respectively. He entered Toyota Motor Corporation in 2014. His research interest includes human–machine interaction of advanced driver assistance systems. He is a member of the JSAE and JSME.

Satoshi Inoue was born in Osaka, Japan, in 1968. He received the B.S. degree in mechanical engineering from Kobe University, Japan, in 1992. He entered Toyota Motor Corporation in 2005. His research interest includes human–machine interaction of advanced driver assistance systems. He is a member of the JSAE.